Human amniotic epithelial cells improve kidney repair in ischemia-reperfusion mouse model of acute kidney injury

Yifei Ren
Peking University First Hospital
Ying Chen
Peking University First Hospital
Xizi Zheng
Peking University First Hospital
Hui Wang
Peking University First Hospital
Xin Kang
Peking University First Hospital
Jiawei Tang
Peking University First Hospital
Lei Qu
Peking University First Hospital
Xiaoyan Shao
Shanghai iCELL Biotechnology Co Ltd
Suxia Wang
Peking University First Hospital
Shuangling Li
Peking University First Hospital
Gang Liu
Peking University First Hospital
Li Yang (li.yang@bjmu.edu.cn)
Peking University First Hospital https://orcid.org/0000-0002-2528-5087

Research

Keywords: Acute kidney injury, human amnion epithelial cells, exosome, cell therapy, ischemia

Posted Date: June 16th, 2020

DOI: https://doi.org/10.21203/rs.3.rs-28766/v1

Version of Record: A version of this preprint was published on September 23rd, 2020. See the published version at https://doi.org/10.1186/s13287-020-01917-y.

Abstract

Background: Acute kidney injury (AKI) is a common clinical disease with complex pathophysiology and very limited therapeutic choices. This prompts the need for novel therapy targeting multiple aspects of this disease. Human amnion epithelial cells (hAECs) are ideal alternative stem cell source for regenerative medicine. Increasing evidence suggests that hAEC-derived exosomes (hAECs-EXO) may act as novel cell–cell communicators. Accordingly, we assessed the therapeutic potential of hAECs in ischemia reperfusion mouse model of AKI and explored the underlying mechanisms.

Methods: The hAECs were primary cultured and hAECs-EXO were isolated and characterized. An ischemic renal injury mouse model was established to mimic different severity of the kidney injury. Mouse blood creatinine level was used to assess renal function and kidney specimens were processed to detect cell proliferation, apoptosis and angiogenesis. Immune cells infiltration was analyzed by flow cytometry. hAECs-EXO was used to treat hypoxia-reoxygenation (H/R) injured HK2 cells and mouse bone marrow-derived macrophages to evaluate their protective effect in vitro. Furthermore, hAEC exosomes were subjected to liquid chromatography-tandem mass spectrometry for proteomic profiling.

Results: We found that systematically administered hAECs could improve mortality and renal function in IRI mice; decrease the number of apoptotic cells; promote peritubular capillary regeneration and modulate kidney local immune response. However, hAECs showed very low kidney tissue integration. Exosomes isolated from hAECs recapitulated the renal protective effects of their parent cells. In vitro, hAECs-EXO protected HK-2 cells from H/R injury-induced apoptosis and promoted bone marrow-derived macrophage polarization toward M2 phenotype. Proteomic analysis on hAECs-EXO revealed proteins involved in extracellular matrix organization, growth factor signaling pathways, cytokine production and immunomodulation. These findings demonstrated that paracrine of exosomes might be a key mechanism by hAECs mediating kidney functional recovery in AKI.

Conclusions: We first reported hAECs could improve mortality and renal repair in mice with ischemia-reperfusion injury. The anti-apoptotic, pro-angiogenetic, and immunomodulatory capabilities of hAECs at least partially, through paracrine pathways. The renoprotective effects of hAECs-EXO might be a promising clinical therapeutic tool, overcoming the weaknesses and risks associated with the use of native stem cells for patients with AKI.

Introduction

Acute kidney injury (AKI) is a common clinical disorder defined by an abrupt decrease in glomerular filtration[1]. An episode of AKI is often associated with an increased risk of developing chronic kidney disease as well as an increased risk of both short- and long-term mortality [2, 3]. Renal ischemia reperfusion (I/R) is one of the major causes of acute kidney injury (IRI-AKI), leading to its high morbidity and mortality[4]. Ischemia and hypoxia lead to tubular and endothelial necrosis and apoptosis. The tissue damage is exacerbated by the initiated inflammatory response after reperfusion and re-oxygenation of

the kidney[5]. Because of the multifactorial pathophysiological mechanisms, there is no effective pharmacological therapy that prevents the evolution or reverses the injury once established[6]. With an increased incidence of AKI worldwide, there is an urgent need to develop more effective strategies for treating AKI.

In the past few years, stem cell therapy has been widely recognized as a potential treatment strategy for AKI. Human amniotic epithelial cells (hAECs) form the epithelial layer of amniotic membrane. As a stem cell, hAEC has attracted widespread attention in regenerative medicine due to its pluripotency, low mutation frequency, low immunogenicity, low tumorigenicity, rich sources, and no ethical risks[7]. Because of these advantageous characteristics, hAECs have obtained a good outcome after transplantation in many diseases, including lung injury[8], brain injury[9], and hepatic fibrosis[10]. However, it is unclear whether hAECs can promote AKI recovery.

Stem cell therapy was observed to have beneficial renal protection under a variety of kidney pathologies, yet differentiation of stem cells into enough number of cells to reconstitute renal parenchymal organs was undetected [11, 12]. Therefore, studies have increasingly focused on the paracrine action of stem cells. Exosomes are major extracellular vesicles with a diameter in the range of 40–150 nm produced by multivesicular bodies and are important information carriers regulating both cellular function and gene expression via transferring cargo into recipient cells[13]. Recent studies have reported that hAEC-derived exosomes reduce liver fibrosis[14], restrict lung injury and enhance endogenous lung repair in bleomycin-challenged aged mice[15].

In this study, we aimed to explore whether hAECs or exosomes secreted from hAECs can reduce AKI mortality and improve renal function in an IRI mouse model, and to make a preliminary discussion on the therapeutic mechanisms of hAECs on AKI.

Material And Methods

Mice

Male C57BL/6j mice (9-10 weeks) were purchased from Vital River Laboratory Animal Technology (Beijing, China) [License No. SCXK (Jing) 2016-0011]. All mice were maintained in animal facilities under SPF conditions. All animal experiments were performed with the approval of the Institutional Animal Care and Use Committee of Peking University First Hospital (Approval Number: J201868).

Culture of hAECs

The human amniotic epithelial cells were provided by Shanghai iCELL Biotechnology Co., Ltd (Shanghai, China). Briefly, the human amniotic epithelial cells were isolated from fresh amnion membranes collected from healthy mothers after cesarean deliveries with written and informed consent. The procedure was approved by the Institutional Ethics Committee of the International Peace Maternity and Child Health Hospital, School of Medicine, Shanghai Jiao Tong University (Approval Number: [2014]11). The amnion

was peeled from the collected placentas, then the blood and mucus were washed away with PBS carefully. The collected amnion tissue was then transferred into a 150 ml flask and dissociated with 50 ml trypsin for 30 min at 37℃. The digestive process was ended by adding 50 ml fresh culture medium. The cell suspension was transferred through a 200 mesh stainless steel screen, centrifuged at 650 g for 5min. The cell pellet was then suspended in fresh culture medium. The cells of passage 1 were characterized by checking phenotype under light microscopy and detecting stem cell markers by flow cytometry (Supplementary Fig. 1).

Exosome isolation and characterization

Exosomes were obtained from the supernatants of hAECs through ultracentrifugation according to classical methods reported previously[16]. In brief, the complete culture medium (CM) from hAECs was collected and centrifuged at 2,000 g for 30 minutes and filtered through a 0.22um cell filter (Millipore, Billerica, MA, USA) to remove debris. The cell-free medium was then centrifuged at 20,000 g (Beckman Coulter, USA) for 30min at 4°C to remove micro-vesicles. The supernatants were discarded and the pellets were washed in PBS, after which the suspension was centrifuged at 100,000 g for 70min at 4°C to obtain exosomes. The ultrastructure of the exosomes was analyzed under a transmission electron microscope (Zeiss, Oberkochen, Germany). The protein levels of TSG101, Alix and Flotllin were detected using western blot. To determine the sizes of the purified vesicles, a nanoparticle tracking analysis (NTA) was performed using Zetaview software (Particle Metrix, Meerbusch, Germany).

Induction of AKI

Ischemia for 30-33 minutes at 37°C was induced in both kidneys using the flank approach as previously reported[17]. Sham operations were performed with exposure of both kidneys, but without induction of ischemia. 100μl of cell-free vehicle, hAECs (1×10^6 cells) or hAECs-exosomes (3×10^8 exosomes) was injected into injured mice via tail vein immediately after surgery. The animals were sacrificed for the subsequent experiments on day 1, day 2, day 3 and day 7 post surgery, respectively. All animal procedures were approved by the Institutional Animal Care and Use Committee of Beijing and were performed in accordance with the National Research Council Guide for the Care and Use of Laboratory Animals. Efforts were made to minimize animal suffering and limit the number of animals used in the study.

Plasma creatinine was determined by the picric acid method as previously reported[18]. Kidney tissue sections were fixed with 10% buffered formalin followed by paraffin embedding and stained with periodic acid-Schiff. The degree of tubulointerstitial damage was scored semi-quantitatively by a renal pathologist who was blinded to the experimental groups. The scores were based on a 0 to 4+ scale, according to the percentage of the cortex and medullar junction region affected by loss of brush border and tubular necrosis and/or apoptosis (0 = no lesion, 1+ = <25%, 2+ = >25% to 50%, 3+ = >50% to 75%, 4+ = >75% to <100%,).

RNA extraction, reverse transcription and real-time RT-PCR

A fraction of kidney was harvested and RNA was isolated using TRIzol® reagent following the manufacturer's instructions (Ambion, Thermo Fisher Scientific Inc., Waltham, MA, USA). RNA concentrations were determined by photometric measurements. cDNA was synthesized from 2 μg total RNA using FastKing RT Enzyme (KR118; TIANGEN Biotech, Beijing, China) for real-time RT-PCR. The primers used for PCR analyses were listed in Supplementary Table 1. Real-time PCR reagents were prepared from the SYBR Green PCR Master Mix (FP209; TIANGEN Biotech, Beijing, China), and all PCR analyses were performed on an ABI Vii7 system.

Immunohistochemistry staining

Immunohistochemistry staining of the kidney was performed on paraffin sections. The primary antibodies included rabbit anti-Ki67 (1:400, Cat. No. 9129, Cell Signaling Technology); rabbit anti-CD31 (1:100, Cat. No.28364, Abcam). The slides were then exposed to DAB-labeled secondary antibodies. The staining was examined using microscope (Leica, Germany). The number of positive cells was counted in 7-8 high-powered fields from the outer medulla in each kidney examined. Apoptosis in kidney tissues was detected on paraffin sections by the in situ terminal deoxynucleotidyl transferase–mediated dUTP nick end-labeling (TUNEL) method following the standard protocol (Beyotime, China).

HK-2 cell hypoxia-reoxygenation (H/R)

HK-2 (immortalized human proximal tubular cells) cells were cultured in DMEM(Gibco) with 10% FBS(Gibco) and 1% penicillin and streptomycin (Gibco) under a humidified atmosphere consisting of 5% CO_2 and 95% air at 37 ℃ (control group). Hypoxia-reoxygenation (H/R) injury was introduced by exposing the cells to hypoxic conditions (1% O_2, 5% CO_2 and 94% N_2) for 48h, followed by reoxygenation under normoxic conditions (5% CO_2 and 95% air, reoxygenation) for 24h in DMEM medium with 10% FBS (H/R group). A concentration of 1×10^8/ml hAECs-EXO was added to DMEM culture medium before H/R injury for the H/R+EXO group.

Western blot analysis

Samples were lysed on ice in lysis buffer supplemented with protease inhibitors. Aliquots of cell lysates were boiled in SDS-PAGE sample buffer, fractionated on 12% SDS-PAGE gel, and transferred to PVDF membrane. The membranes were blocked with 5% milk in TBST (Tris-buffered saline, 10 mM Tris-HCl [pH 7.5], 150 mM NaCl, and 0.1% Tween-20) for 1 hour at room temperature and incubated with primary antibodies at 4°C overnight. The following primary antibodies and dilutions were used: rabbit anti-Alix (1:5,000, Cat. No.186429, Abcam), rabbit anti-TSG101 (1:1000, Cat. No.125011, Abcam), rabbit anti-Flotillin (1:5000, Cat. No.133497, Abcam), rabbit anti-CD31(1:500, Cat. No.28364; Abcam), mouse anti-PCNA (1:1000, Cat. No.29, Abcam), rabbit anti-cleaved caspase3(1:1000, Cat. No.9661, Cell Signaling Technology), rabbit anti-Caspase3(1:1000, Cat. No.9662, Cell Signaling Technology) and anti-GAPDH (1:10000; Beyotime). Then, the membranes were incubated with horseradish peroxidase-conjugated secondary antibodies (1:1000; Beyotime) for 1 hour at room temperature. Visualization of the blots was performed using the standard protocol for electrochemiluminescence (ECL; Santa Cruz Biotechnology).

The relative intensity of the protein bands was quantified by digital densitometry using ImageJ software (NIH, Bethesda, MD, USA). The level of glyceraldehyde 3-phosphate dehydrogenase (GAPDH) was used as an internal standard.

Cytokine and chemokine quantification

Bio-Plex Pro Mouse Cytokine 23-plex Assay (Bio-Plex Pro, Bio-Rad Laboratories, Inc.) was used to quantify the concentrations of 23 cytokines and chemokines in mouse kidneys: IL1α, IL1β, IL2, IL3, IL4, IL5, IL6, IL9, IL10, IL12/p40, IL12/p70, IL13, IL17A/CTLA8, Eotaxin/CCL11, G-CSF, GM-CSF, IFNγ, KC/CXCL1, MCP-1 (MCAF)/CCL2, MIP-1α/CCL3, MIP-1β/CCL4, RANTES/CCL5, TNFα. Measurements were made on MAGPIX multiplexing instrument (Luminex Corporation, Austin, TX, United States). The manufacturer's recommended quality control procedures were followed to ensure validity.

Flow cytometry

Mice were anesthetized, sacrificed, and perfused with ice-cold PBS via the left ventricle for 2 minutes. Kidneys were minced and incubated with collagenase type IA (1mg/ml, Sigma-Aldrich) in DMEM/F12 for 25 minutes at 37°C with constant shaking. Digestion was stopped by the addition of ice-cold FBS. The digested kidney tissue suspension was passed through a 100-μm cell strainer (Thermo Fisher) and centrifuged at 1,000 g for 5 minutes at 4°C. The pellet was then incubated with ACK Lysing Buffer (0.15 M NH4Cl, 10 mM KHCO3, and 0.1 mM Na2 EDTA) for 5 minutes at room temperature to remove red blood cells, and centrifuged twice at 1,000 g for 5 minutes at 4°C. The pellet was then washed with PBS. Cells were incubated with F4/80 (PE/cy7, Cat. No.123113, BioLegend) and CD206 (AF647, Cat. No. 141712, BioLegend) antibodies. Data were acquired using BD FACSVerse and analyzed using FlowJo software.

Culture of mouse bone marrow-derived macrophage

L929 fibrosarcoma cells were cultured in RPMI 1640 (Gibco, UK) medium supplemented with 10% fetal bovine serum at 37°C in humidified air containing 5% CO_2 for 48h. L929 supernatant ($1x10^6$ cells/mL) was collected and filtrated through 0.22 μm Millipore membrane and used in macrophage cultures (L929 sup).

Bone marrow-derived macrophages were isolated and cultured as described previously[19]. In brief, bone marrow cells were collected from the tibia and femur of 8 weeks old C57BL/6J mice. Cells were cultured in L929 conditioned medium (RPMI-1640 with 10% heat inactivated fetal bovine serum, 15% L929 sup, and 100 U/mL penicillin-streptomycin) and allowed to attach for 2 days. A fraction of cells was collected before polarization. The rest of cells were continued to culture in hAECs-EXO conditioned medium (RPMI-1640 with 10% heat inactivated fetal bovine serum,$1x10^8$ exosomes/ml, and 100 U/mL penicillin-streptomycin) for 7 days. On day 8, the media was removed and the cells were lysed in TRIzol® reagent and quantified M1 and M2 macrophage marker gene expression by reverse transcription-PCR. The primers used for PCR analyses were listed in Supplementary Table 1.

Shotgun proteomics followed by label-free quantification

Peptide preparation for proteomic analysis was performed as described previously[20]. Briefly, 300ug exosome proteins isolated from hAECs were used to perform the analysis with triplicates. Proteins were separated using 4–15% Mini-PROTEAN® TGX™ Precast Protein Gel (BioRad, Hercules, CA, USA), stained with Coomassie Brilliant Blue R-250 staining solution (BioRad, Hercules, CA, USA). Total proteins resolved using mono-dimensional gel electrophoresis was subjected to protein-in-gel digestion. The peptides of each sample were desalted by a C_{18} Cartridge, concentrated by vacuum centrifugation and reconstituted in 40 uL of 0.1% formic acid.

The MS experiments were performed on a Q-Exactive HF Hybrid quadrupole-Orbitrap mass spectrometer (Thermo Fisher Scientific, Hemel Hempstead, UK) coupled to an Easy nLC nano-liquid chromatography (Thermo Fisher Scientific, Hemel Hempstead, UK). The desalted peptides were separated on a 15cm long separation column with an inner diameter of 50 um (Acckaim PepMap RSLC, nano viper, P/N164943, Thermo Fisher Scientific, USA) using gradient of buffer A (Ultrapure water, 0.1% formic acid) and buffer B (Acetonitrile, 0.1% formic acid) at a flowrate of 300 nL min-1. The chromatographic gradient was set to provide a linear increase from 3% to 80% buffer B in 110 min, for a total run time of 120 min. MS data was acquired on data dependent mode dynamically choosing the top ten most abundant precursor ions from the survey scan (350-1800 m/z) for fragmentation and MS/MS analysis. Precursors with a charged state of +1 were rejected and the dynamic exclusion duration was set as 25 s. MS raw data were processed using MaxQuant software version 1.5.5.1 according to the standard workflow with the built-in search engine Andromeda[21]. Proteins were identified by searching against the Uniprot human reference proteome (Uniprot_HomoSapiens_20386_20180905) database. Carbamidomethylation of cysteines was set as fixed modification, while protein N-terminal acetylation and methionine oxidation were defined as variable modifications for peptide search. The false discovery rates (FDR) for peptide and protein identifications were set to 0.01%. A maximum of two missed cleavages were allowed for tryptic digestion. The MaxLFQ label-free quantitation method[22] with retention time alignment and match-between-runs feature in MaxQuant was applied to extract the maximum possible quantification information. Protein abundance was calculated based on normalized spectral intensity (LFQ intensity).

The gene ontology (GO) annotation in categories such as cellular component, biological process, molecular functions of the significantly expressed proteins was carried out using DAVID functional enrichment analysis tool (https://david.ncifcrf.gov/).

Statistical analysis

Statistical analysis was performed using SPSS 25.0 statistical software (SPSS, Chicago, IL). Normally distributed variables are expressed as mean ± standard deviation and compared using a t-test. Non-normally distributed non-parametric variables are expressed as median and interquartile range and are compared between groups using the Mann-Whitney U test. All P values were two-tailed, and $P < 0.05$ was considered statistically significant.

Results

hAECs ameliorated acute renal IRI

We established an ischemic renal injury mice model by changing the clamping time of the bilateral renal pedicle to control the severity of the injury. The seven-day mortality rate in the 33min-IRI group reached to 90% (Fig. 1a) (n = 21), and the blood creatinine level on the first day after surgery was 1.95 ± 0.15mg / dl (Fig. 1b), which was in line with the characteristics of clinically severe AKI. There was no death in the 30min-IRI group (Fig. 1a), and the postoperative day 1 serum creatinine was 0.97 ± 0.3mg / dl, which was corresponding to clinically moderate AKI (Fig. 1b). The mice subjected to renal IRI showed pronounced renal pathological damage compared to mice in the sham group. The main features were tubular cell swelling, widespread tubular dilation and degeneration, nuclear condensation, and inflammatory cell infiltration (Fig. 1c). Therefore, we successfully established a mouse model of IRI-AKI. Due to the significant natural death of the 33min-IRI group, the severe AKI model was used to observe the seven-day mortality of mice, while the 30min-IRI group of moderate AKI was mainly used to assess mouse kidney damage and subsequent mechanism study.

We next examined the effects of hAECs on IRI renal damage. Injection of hAECs reduced the seven-day mortality rate from 90% to 47.4% ($p < 0.05$) in the 33min-IRI severe AKI group (Fig. 1d). Serum creatinine levels were decreased in hAECs group on day 1 and day 2 post-surgery (Fig. 1e). The proportion of necrotic and damaged tubules tended to be lower in the cortex and outer medullar regions of the hAECs treated group than in the Vehicle control (Fig. 1 f and g). These findings indicate that hAECs can promote renal function and enhance mice survival in IRI-AKI.

hAECs-EXO recapitulated hAECs' protective effect on renal IRI

We examined hAECs organ engraftment after transplantation and found very low kidney tissue integration of hAECs from the beginning of injection till 7 days post injection despite a positive therapeutic signal in the IRI-AKI mice (Supplementary Figure2). Except the direct repopulation to the injured tissues, stem cells also exerted their therapeutic effect by paracrine/endocrine of extracellular vesicles such as exosomes[23]. We isolated exosomes from hAEC conditioned medium and tested their effects on IRI-AKI. The morphological assessment revealed the typical cup-shaped morphology of exosomes as determined by transmission electron microscopy (Fig. 2a). Size analysis using a nanoparticle tracking system showed a peak size of 50-150 nm (Fig. 2b). Western blot results showed the presence of exosomal markers, including Flotillin, TSG101 and Alix in the hAEC exosomes (Fig. 2c).

As shown in Fig. 2d, injection of hAECs-EXO reduced the seven-day mortality rate from 81.8% to 50% ($p < 0.05$) in 33min-IRI group. In 30min-IRI group, serum creatinine levels were significantly decreased ($p<0.05$ on post-surgery day 1 and day 2) (Fig. 2e). Renal tubule necrosis was also reversed after hAECs-EXO injection (Fig. 2 f and g).

hAECs and hAECs-EXO protected kidney from AKI by reducing apoptosis and stimulating cell proliferation

On ischemic insults, tubular cells often undergo apoptosis or necrosis. When TUNEL-stained kidney tissues were observed by fluorescence microscopy, the number of apoptotic cells in the IRI group was significantly increased compared with that in the sham group (Fig. 3a). However, as shown in Fig. 3b, hAECs or hAECs-EXO treatment significantly decreased the number of apoptotic cells. Moreover, in vitro, HK-2 cells were cultured in a hypoxic environment to simulate ischemia within the tissue, and proteins from the HK-2 cells treated with or without hypoxia-reoxygenation (H/R) injury were collected. Western blot analysis showed that the expression level of apoptosis-related marker cleaved caspase-3 in the H/R group was significantly higher than that in the control group, while hAECs-EXO treatment significantly suppressed cleaved casapase-3 expression (Fig. c and d).

Meanwhile, hAECs and hAECs-EXO stimulated dramatic tubular cell proliferation two days after surgery as shown by anti-Ki67 staining (Fig 3e and f). Similarly, in H/R stimulated HK-2 cells, the expression of PCNA was significantly higher in hAECs-EXO treated group than H/R group (Fig. 3 g and h). Taken together, these observations demonstrated that hAECs exosomes enhanced cell proliferation and attenuated apoptosis in renal epithelial cells under H/R injury.

hAECs and hAECs-EXO promoted angiogenesis

The tubular injuries in AKI are accompanied by renal vascular impairment. We next investigated the change of peritubular capillaries (PTCs) in IRI kidneys by immunohistochemistry and Western blot analysis using PTC endothelial cell marker, CD31. CD31+ capillaries were found to be intact in the sham kidney. Ischemia induced significant PTCs loss in the kidneys during the 7-day course of reperfusion ($p < 0.05$). However, the number of microvascular capillaries was highly increased by hAECs transplantation or hAECs-EXO administration ($p<0.05$) post ischemic injury (Fig. 4 a-d). We also determined the mRNA levels of the angiogenesis-related genes (*Egf*, *Fgf, Hgf, Igf-1, Pdgf,* and *Vegf*) in the IRI kidneys. The expression of these regeneration markers was very weak in sham kidneys and IRI induced a slight increase in the gene expression. hAECs and hAECs-EXO treatment significantly upregulated the expression of these genes, with only no obvious difference in *Egf* expression between vehicle control group and hAECs or hAECs-EXO treatment groups (Fig. 4e).

hAECs and hAECs-EXO increased M2 macrophage infiltration with a concomitant modulation of inflammatory cytokines

Stem cell therapy has been reported to prevent renal injuries via immune regulation[24,25]. Macrophages are important immune cells with high heterogeneity and plasticity, and the imbalance of M1/M2 macrophages phenotypes contributes to the inflammation or tissue repair in acute kidney injury. Ischemia reperfusion promoted immune cell infiltration into the kidney as shown by the increased percentage of macrophage compared to the sham group (Fig.5a). A continuous increase of macrophage population was observed during the 7-day course of reperfusion in hAECs and hAECs-EXO treated kidney (Fig. 5b), in consistent with the high levels of macrophage attractive chemokines in local kidney (Fig.5c).

The phenotype of local macrophages was determined by flow cytometry (Fig. 6a). I/R animals exhibited prominent infiltration of CD206+/F4/80+ M2 type macrophages in the kidneys on day 2 and afterwards after hAECs transplantation or hAECs-EXO administration (Fig. 6b). Concomitantly, postischemic kidneys of the hAEC or hAECs-EXO-treated groups expressed higher levels of anti-inflammatory cytokines such as IL4 and IL13, and lower levels of proinflammatory cytokines such as IFNγ and TNFα, than those of the vehicle-treated group (Fig. 6c). In vitro, using hAECs-EXO as supplement to culture bone marrow-derived macrophages for 7 days, the gene expression of M2 markers including *Cd206*, *Cd163*, *Il4r*α, and *Arg*1 was significantly increased, with a downregulation of gene expression of M1 markers such as *Cd86*, *Ifn*γ, *Tnf*α and *iNos* (Fig. 6d). Thus, we postulated that hAECs could alleviate IRI probably through promoting M2 macrophage polarization and inhibiting the systemic inflammation.

Proteomic profiling of hAECs-EXO

Above data revealed that hAEC-derived exosomes displayed renal protective functions similar to parent cells, indicating the paracrine pathway played an important role in the process of hAEC-mediated kidney tissue functional recovery. A comprehensive analysis of the proteome on hAECs-EXO allowed an overall identification of 171 proteins (Supplementary table 1). The functional annotation of these proteins was performed using DAVID functional enrichment analysis tool. Predictably, a large proportion of exosome proteins was annotated as either of extracellular or membrane origin, with a sizable contribution to the cytosol and ER lumen (Fig. 7a). The molecular functions of these exosome proteins were mainly involved in protein binding, integrin binding, heparin binding, cadherin binding as well as extracellular matrix structural constituent (Fig. 7b). The biological process category showed “extracellular matrix organization”, “cell adhesion”, “regulation of complement activation”, “leukocyte migration”, “innate immune response”, as well as “angiogenesis” and “positive regulation of cell proliferation” as the most enriched terms (Fig. 7c).

We next examined the detailed function of these 171 hAEC exosome proteins in Uniprot protein bank (http://www.uniprot.org) and found a large population of proteins were extracellular matrix (ECM) constituents (FN1, COL5A1, COL1A2, LAMA3, COL12A1, LAMB3, LAMC2, COL3A1, LAMC1, COL1A1, LAMB1, FBN1, COL7A1, VTN, LAMA5, COL6A1, FBLN1, LAMB2, FBN2, COL6A3) or Matricellular Proteins (TNXB, THBS1, THBS3, and OLFML3). We also found a series of proteins were involved in proliferation/apoptosis and angiogenesis. These signaling pathways included integrin signaling (ITGB3, ITGB6, ITGAV, ITGA6, ITGA2), IGF signaling (IGFBP2, IGF2), HGF signaling (HGFAC), TGFβ signaling (TGFBI, LTBP1, BMP1), Wnt signaling (DKK3, SFRP1, LRP1) and programmed cell death pathway (PDCD6IP). SPARC, SERPINE1, NID2, MYLK, CCDC80, TIMP1, WDR1 and the complement components (C3, C6, C4B, C1R, C1QB, C8B, C2, C5) were reported to participate in cell migration, cytokine production and inflammation. Taken together, hAECs-EXO might serve as important carriers with anti-apoptotic, pro-angiogenic and immunomodulatory proteins that could target multiple aspects of the IRI damage and ameliorate the acute kidney tissue injury.

Discussion

Acute kidney injury is the rapid onset of decreased kidney function that ultimately increases mortality and morbidity. Despite the ever-increasing prevalence of acute kidney disease, there is a lack of potential therapeutic agents, leaving us with the option of costlier replacement therapies. In recent years, stem cell therapy has drawn much attention for the treatment of AKI [26]. As a main player, MSCs derived from different sources like adipose, bone-marrow and human umbilical cord have shown renoprotective effects in several models of toxin or IRI-induced AKI [27–29]. Meanwhile, numerous controversies have yet arisen regarding safety, cost, availability, and ethical considerations of MSCs[30]. In seeking of alternative cell sources, human amniotic epithelial cells are one of the most promising. In the current study, we observed a decrease of mortality rate after hAEC treatment in our severe IRI-AKI mice model.

Ischemia-reperfusion injuries leading to AKI have been associated with accumulation of reactive oxygen species (ROS) and apoptosis, loss of peritubular capillaries and migration of pro-inflammatory immune cells to the damage tissue[4, 31]. In our study, we demonstrated that hAEC therapy could effectively reduce kidney injury in animal model of IRI induced AKI. Intravenous injection of hAECs attenuated the loss of peritubular capillaries and tubular cell apoptosis and necrosis, and promoted cell proliferation in the IRI injured kidney. hAECs reprogramed macrophages to shift from a pro-inflammatory M1 to anti-inflammatory M2 state. This shift was associated with the increased levels of IL4, IL13 and decreased levels of TNFα and IFNγ, which in turn helped to reduce the inflammatory response. Taken together, these anti-inflammatory, anti-apoptotic, and pro-angiogenetic effects of hAECs were associated with both the rapid recovery of kidney function and the enhanced survival in the mice with IRI kidney injury.

It was originally believed that stem cells provided a therapeutic basis for regeneration by engrafting at the site of injury via transdifferentiation. However, further investigation revealed that engraftment of stem cells to the site of injury was very rare and therefore was not likely to be the sole cause of regeneration after AKI[32]. In our case, we found very few kidney tissue integration of hAECs after transplantation. The majority of hAECs were concentrated in the lung and heart. Growing evidence in regenerative medicine supports the hypothesis that stem cells exert their therapeutic effect by a paracrine/endocrine manner rather than a direct repopulation of the injured tissues [23]. Exosomes secreted from stem cells could act as major transporters in cell-cell communication to deliver bioactive molecules from original cells to the recipient cells[33]. It has been reported that hAEC-derived exosomes can restore ovarian function in chemotherapy-induced premature ovarian failure by transferring microRNAs against apoptosis[34]. In our study, we found that injection of exosomes derived from hAECs recapitulated hAECs' protective effects on renal ischemia reperfusion injury, limiting apoptosis, enhancing proliferation, regulating angiogenesis and immune response, and thus promoting kidney repair.

We characterized the molecular compositions of hAECs-EXO by proteomic approach to find out the specific mechanisms of hAEC-based therapy in AKI. Cellular processes including "extracellular matrix organization", "cell adhesion", "leukocyte migration" as well as "angiogenesis" and "positive regulation of cell proliferation" were enriched in hAECs-EXO. Proteins involved in the IGF signaling, HIF signaling, Integrin signaling, Wnt signaling, and TGFβ signaling were detected in hAECs-EXO. ECM proteins are also abundant in hAECs-EXO. It has been shown that ECM processing and cell-ECM interactions are major

determinants in the regulation of signaling pathways that drive kidney repair [35, 36]. In addition to the classical ECM structural proteins, we found that several Matricellular Proteins (MCPs) such as TNXB, THBS1, THBS3 were detected in hAEC-EXO with high abundance. MCPs are ECM bound nonstructural proteins that interact with integrins, growth factor receptors, and growth factors to modulate their function and activity[37, 38]. In our proteomic analysis, Tenascin X (TNXB) as a typical matricellular protein stands out. An in vitro study has shown that TNX physically interacts with VEGF-B and enhances the ability of VEGF-B to stimulate endothelial cell proliferation[39], suggesting a role for TNXB in the regulation of angiogenesis. It was found that in normal kidney tenascin expression was limited to the medullary interstitium[40]. Chen *et.al.* reported that Tenascin-C (TNC), a member of the tenascin family, was specifically induced at sites of injury and recruited Wnt ligands, thereby creating a favorable microenvironment for tubular repair and regeneration after ischemia reperfusion-induced AKI[41]. Thus, it would be interesting to explore the in vivo role of TNXB on kidney regeneration in IRI models, leading to an elucidation of the molecular mechanism of hAECs therapy for AKI.

Conclusion

In summary, the above findings advance our knowledge of the therapeutic potential of hAECs in ischemia reperfusion-induced AKI mouse model, pointing to hAECs as an attractive candidate for promoting renal tissue repair, possibly through the limitation of apoptosis, promotion of angiogenesis and immunomodulation. Our data also demonstrate the renoprotective effects of hAEC-derived exosomes, which might be a promising clinical therapeutic tool, overcoming the weaknesses and risks associated with the use of native stem cells for patients with AKI.

Declarations

Ethics approval and consent to participate

Human amniotic epithelial stem cells were isolated from fresh amnion membranes collected from healthy mothers after cesarean deliveries with written and informed consent. The procedure was approved by the Institutional Ethics Committee of the International Peace Maternity and Child Health Hospital, School of Medicine, Shanghai Jiao Tong University (Approval Number: [2014]11).

All animal experiments were performed with the approval of the Institutional Animal Care and Use Committee of Peking University First Hospital (Approval Number: J201868)

Consent for publication

Not applicable

Availability of data and materials

The datasets used and/or analyzed during the current study are available from the corresponding author on reasonable request.

Competing interests

Li Yang has a patent pending for the use of hAECs in repair of the injured kidney after AKI. Shanghai iCELL Biotechnology company declared no potential conflicts of interest with respect to the research, authorship, and/or publication of this article.

Funding

This study was supported by grants from the National Natural Science Foundation of China (No.91742205 and No.81625004), the Beijing Young Scientist Program (BJJWZYJH01201910001006), the National Science and Technology Major Projects for "Major New Drugs Innovation and Development" of China (No.2017ZX09304028), and Peking University Clinical Scientist Program by the Fundamental Research Funds for the Central Universities.

Authors' contributions

Yifei Ren and Ying Chen: conception and design, provision of study material, collection and assembly of data, data analysis and interpretation, manuscript writing, final approval of manuscript; Xizi Zheng, Hui Wang, Xin Kang, Lei Qu and Xiaoyan Shao: collection and/or assembly of data; Jiawei Tang: financial support, administrative support. Suxia Wang, Shuangling Li and Gang Liu: conception and design, final approval of manuscript; Li Yang: conception and design, data analysis and interpretation, manuscript writing, final approval of manuscript.

Acknowledgements

Not applicable

Authors' information (optional)

References

1. Bellomo R, Kellum JA, Ronco C. Acute kidney injury. Lancet. 2012;380(9843):756–66.
2. Chertow GM, Burdick E, Honour M, et al. Acute kidney injury, mortality, length of stay, and costs in hospitalized patients. J Am Soc Nephrol. 2005;16(11):3365–70.
3. Coca SG, Yusuf B, Shlipak MG, et al. Long-term risk of mortality and other adverse outcomes after acute kidney injury: a systematic review and meta-analysis. Am J Kidney Dis. 2009;53(6):961–73.
4. Sharfuddin AA, Molitoris BA. Pathophysiology of ischemic acute kidney injury. Nat Rev Nephrol. 2011;7(4):189–200.
5. Reuter S, Mrowka R. Acute kidney injury. Acta Physiol (Oxf). 2015;215(2):73–5.

6. Chatterjee PK. Novel pharmacological approaches to the treatment of renal ischemia-reperfusion injury: a comprehensive review. Naunyn Schmiedebergs Arch Pharmacol. 2007;376(1–2):1–43.
7. Miki T. Stem cell characteristics and the therapeutic potential of amniotic epithelial cells. Am J Reprod Immunol. 2018;80(4):e13003.
8. Cargnoni A, Piccinelli EC, Ressel L, et al. Conditioned medium from amniotic membrane-derived cells prevents lung fibrosis and preserves blood gas exchanges in bleomycin-injured mice-specificity of the effects and insights into possible mechanisms. Cytotherapy. 2014;16(1):17–32.
9. Kakishita K, Elwan MA, Nakao N, et al. Human amniotic epithelial cells produce dopamine and survive after implantation into the striatum of a rat model of Parkinson's disease: a potential source of donor for transplantation therapy. Exp Neurol. 2000;165(1):27–34.
10. Manuelpillai U, Tchongue J, Lourensz D, et al. Transplantation of Human Amnion Epithelial Cells Reduces Hepatic Fibrosis in Immunocompetent CCl4-Treated Mice [in English]. Cell Transplant. 2010;19(9):1157–68.
11. Toegel F, Hu ZM, Weiss K, et al. Administered Mesenchymal Stem Cells Protect against Ischemic Acute Renal Failure through Paracrine and Anti-Inflammatory Mechanisms [in English]. Nephrology 2005;10:A343-A344.
12. Duffield JS, Park KM, Hsiao LL, et al. Restoration of tubular epithelial cells during repair of the postischemic kidney occurs independently of bone marrow-derived stem cells [in English]. J Clin Invest. 2005;115(7):1743–55.
13. Keerthikumar S, Chisanga D, Ariyaratne D, et al. ExoCarta: A Web-Based Compendium of Exosomal Cargo [in English]. J Mol Biol. 2016;428(4):688–92.
14. Alhomrani M, Correia J, Hodge A, et al. Extracellular vesicles derived from human amnion epithelial cells reduce liver fibrosis through effects on hepatic stellate cells and macrophages [in English]. Hepatology. 2016;64:212a-212a.
15. Murphy S, Lim R, Dickinson H, et al. Human Amnion Epithelial Cells Prevent Bleomycin-Induced Lung Injury and Preserve Lung Function [in English]. Cell Transplant. 2011;20(6):909–23.
16. Cantaluppi V, Gatti S, Medica D, et al. Microvesicles derived from endothelial progenitor cells protect the kidney from ischemia-reperfusion injury by microRNA-dependent reprogramming of resident renal cells [in English]. Kidney Int. 2012;82(4):412–27.
17. Park KM, Byun JY, Kramers C, et al. Inducible nitric-oxide synthase is an important contributor to prolonged protective effects of ischemic preconditioning in the mouse kidney [in English]. J Biol Chem. 2003;278(29):27256–66.
18. Zahedi K, Revelo MP, Barone S, et al. Stathmin-deficient mice develop fibrosis and show delayed recovery from ischemic-reperfusion injury [in English]. Am J Physiol-Renal. 2006;290(6):F1559–67.
19. Manzanero S. Generation of mouse bone marrow-derived macrophages. Methods Mol Biol. 2012;844:177–81.
20. Rappsilber J, Mann M, Ishihama Y. Protocol for micro-purification, enrichment, pre-fractionation and storage of peptides for proteomics using StageTips [in English]. Nat Protoc. 2007;2(8):1896–906.

21. Tyanova S, Temu T, Cox J. The MaxQuant computational platform for mass spectrometry-based shotgun proteomics [in English]. Nat Protoc. 2016;11(12):2301–19.
22. Cox J, Hein MY, Luber CA, et al. Accurate Proteome-wide Label-free Quantification by Delayed Normalization and Maximal Peptide Ratio Extraction, Termed MaxLFQ [in English]. Mol Cell Proteomics. 2014;13(9):2513–26.
23. Grange C, Skovronova R, Marabese F, et al. Stem Cell-Derived Extracellular Vesicles and Kidney Regeneration. Cells 2019;8(10).
24. Tseng W, Hung S, Chien C, et al. Hypoxia-Preconditioned Mesenchymal Stem Cells Mitigate Renal Ischemia-Reperfusion Injury by Modulating M2 Macrophage Subsets and Suppressing Oxidative Stress [in English]. Cytotherapy 2018;20(5):S54-S54.
25. Yuan YJ, Li L, Zhu LL, et al. Mesenchymal stem cells elicit macrophages into M2 phenotype via improving transcription factor EB-mediated autophagy to alleviate diabetic nephropathy [in English]. Stem Cells 2020.
26. Barnes CJ, Distaso CT, Spitz KM, et al. Comparison of stem cell therapies for acute kidney injury. Am J Stem Cells. 2016;5(1):1–10.
27. Zhang JB, Wang XQ, Lu GL, et al. Adipose-derived mesenchymal stem cells therapy for acute kidney injury induced by ischemia-reperfusion in a rat model. Clin Exp Pharmacol Physiol. 2017;44(12):1232–40.
28. Geng Y, Zhang L, Fu B, et al. Mesenchymal stem cells ameliorate rhabdomyolysis-induced acute kidney injury via the activation of M2 macrophages. Stem Cell Res Ther. 2014;5(3):80.
29. Fang TC, Pang CY, Chiu SC, et al. Renoprotective effect of human umbilical cord-derived mesenchymal stem cells in immunodeficient mice suffering from acute kidney injury. PLoS One. 2012;7(9):e46504.
30. Musial-Wysocka A, Kot M, Majka M. The Pros and Cons of Mesenchymal Stem Cell-Based Therapies [in English]. Cell Transplant. 2019;28(7):801–12.
31. Zuk A, Bonventre JV. Acute Kidney Injury. Annu Rev Med. 2016;67:293–307.
32. Phinney DG, Prockop DJ. Concise review: mesenchymal stem/multipotent stromal cells: the state of transdifferentiation and modes of tissue repair–current views. Stem Cells. 2007;25(11):2896–902.
33. Hur YH, Cerione RA, Antonyak MA. Extracellular vesicles and their roles in stem cell biology [in English]. Stem Cells 2020.
34. Zhang Q, Sun J, Huang Y, et al. Human Amniotic Epithelial Cell-Derived Exosomes Restore Ovarian Function by Transferring MicroRNAs against Apoptosis. Mol Ther Nucleic Acids. 2019;16:407–18.
35. Wynn TA, Ramalingam TR. Mechanisms of fibrosis: therapeutic translation for fibrotic disease [in English]. Nat Med. 2012;18(7):1028–40.
36. Liu YH. Renal fibrosis: New insights into the pathogenesis and therapeutics [in English]. Kidney Int. 2006;69(2):213–7.

37. Bornstein P. Matricellular proteins: an overview [in English]. J Cell Commun Signal. 2009;3(3–4):163–5.
38. Murphy-Ullrich JE, Sage EH. Revisiting the matricellular concept [in English]. Matrix Biol. 2014;37:1–14.
39. Ikuta T, Ariga H, Matsumoto K. Extracellular matrix tenascin-X in combination with vascular endothelial growth factor B enhances endothelial cell proliferation [in English]. Genes Cells. 2000;5(11):913–27.
40. Truong LD, Foster SV, Barrios R, et al. Tenascin is an ubiquitous extracellular matrix protein of human renal interstitium in normal and pathologic conditions [in English]. Nephron. 1996;72(4):579–86.
41. Chen SQ, Fu HY, Wu SZ, et al. Tenascin-C protects against acute kidney injury by recruiting Wnt ligands [in English]. Kidney Int. 2019;95(1):62–74.

Figures

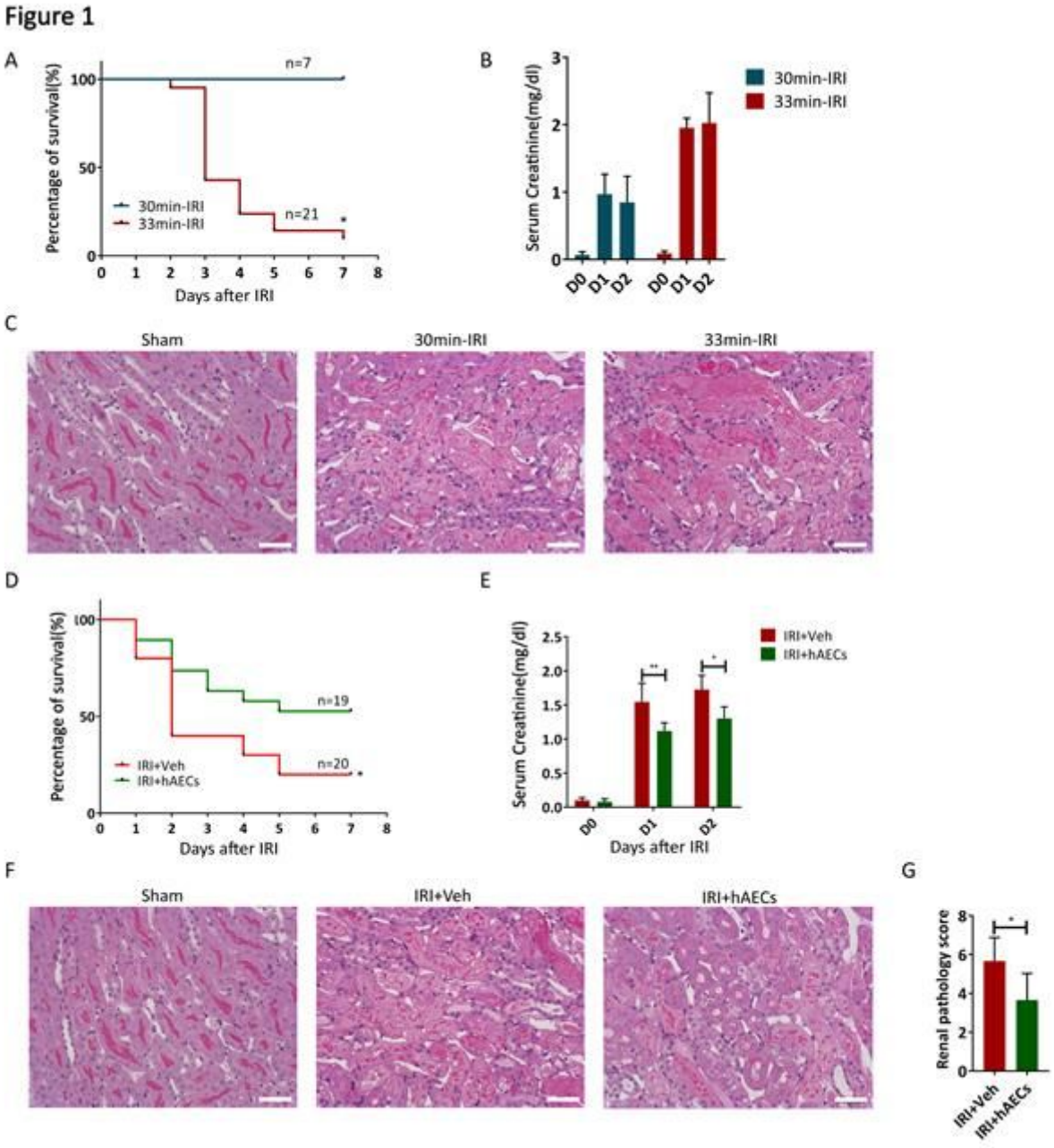

Figure 1

hAECs ameliorated acute renal IRI. A, 7-days mortality rate in IRI mice with 30 minutes (30min-IRI, n=7) or 33 minutes (33min-IRI, n=21) ischemia. *P < 0.05. B, Serum creatinine concentrations at day 1 and day 2 post-surgery in 30min-IRI group and 33min-IRI group. C, Representative micrographs of renal histology of sham, 30min-IRI group and 33min-IRI group at day 1 after surgery. Scale bar: 25μm. D, 7-days mortality rate in IRI mice with 33 minutes ischemia followed by vehicle (n=19) or hAECs (n=20) injection. *P < 0.05. E, Serum creatinine concentrations in mice injected with vehicle alone or treated with hAECs. *P < 0.05 vs IRI+Veh group, **P <0.01 vs IRI+Veh group. F, Periodic acid-Schiff staining of postischemic kidneys on day 1 after IRI. Scale bar: 25μm. G, Renal pathological scores representing the degree of tubulointerstitial

damage. *P < 0.05 vs IRI+Veh group. IRI+Veh: IRI mice injected with vehicle alone; IRI + hAECs: IRI mice injected with 1x106 hAECs right after surgery. Data are shown as mean (SD).

Figure 2

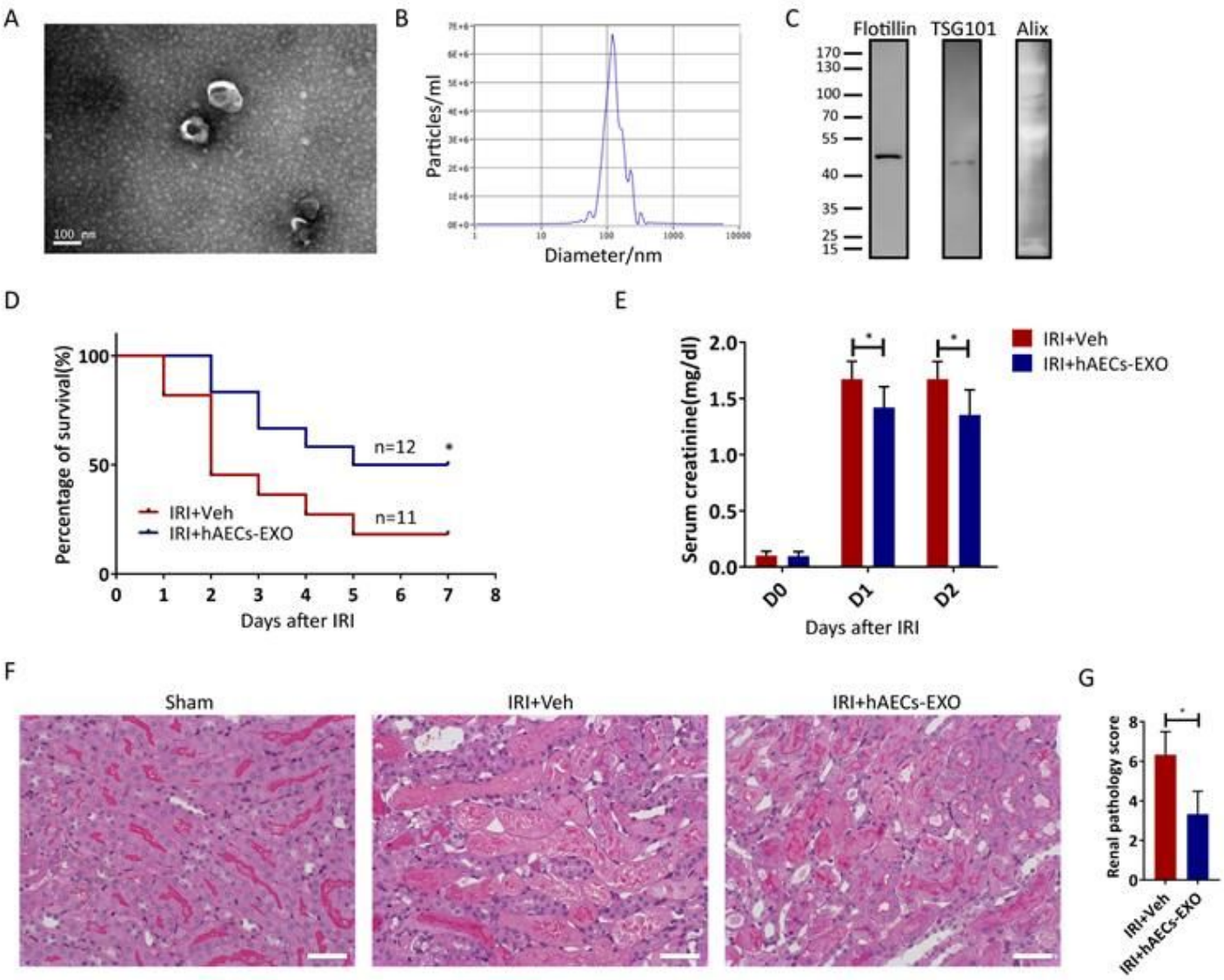

Figure 2

Effects of intravenous injection of hAECs-EXO in mice with IRI-induced AKI. A, Morphology of hAECs exosomes under transmission electron microscopy. Scale bar, 100 nm. B, Mean diameter of hAECs exosomes analyzed by nanoparticle tracking system (NTA). Approximately 1.6 × 1010 particles were measured by NTA in hAECs exosomes, which came from a total of 5 × 107 hAECs. C, Western blot detection of the exosome markers Flotillin, TSG101, and Alix. D, 7-days mortality rate after IRI in mice injected with vehicle (IRI+Veh, n=11) or hAECs-EXO (IRI+hAECs-EXO, n=12). *P < 0.05. E, Serum creatinine concentrations in mice injected with vehicle alone (IRI+Veh) or hAECs-EXO at day 0, day 1 and day 2 after IRI. *P < 0.05 vs IRI+Veh group. F, Periodic acid-Schiff staining of postischemic kidneys at day 1 after IRI

in different groups as indicated. Scale bar: 25μm. G. Renal pathological scores representing the degree of tubulointerstitial damage. *P < 0.05 vs IRI+Veh group. Data are shown as mean (SD).

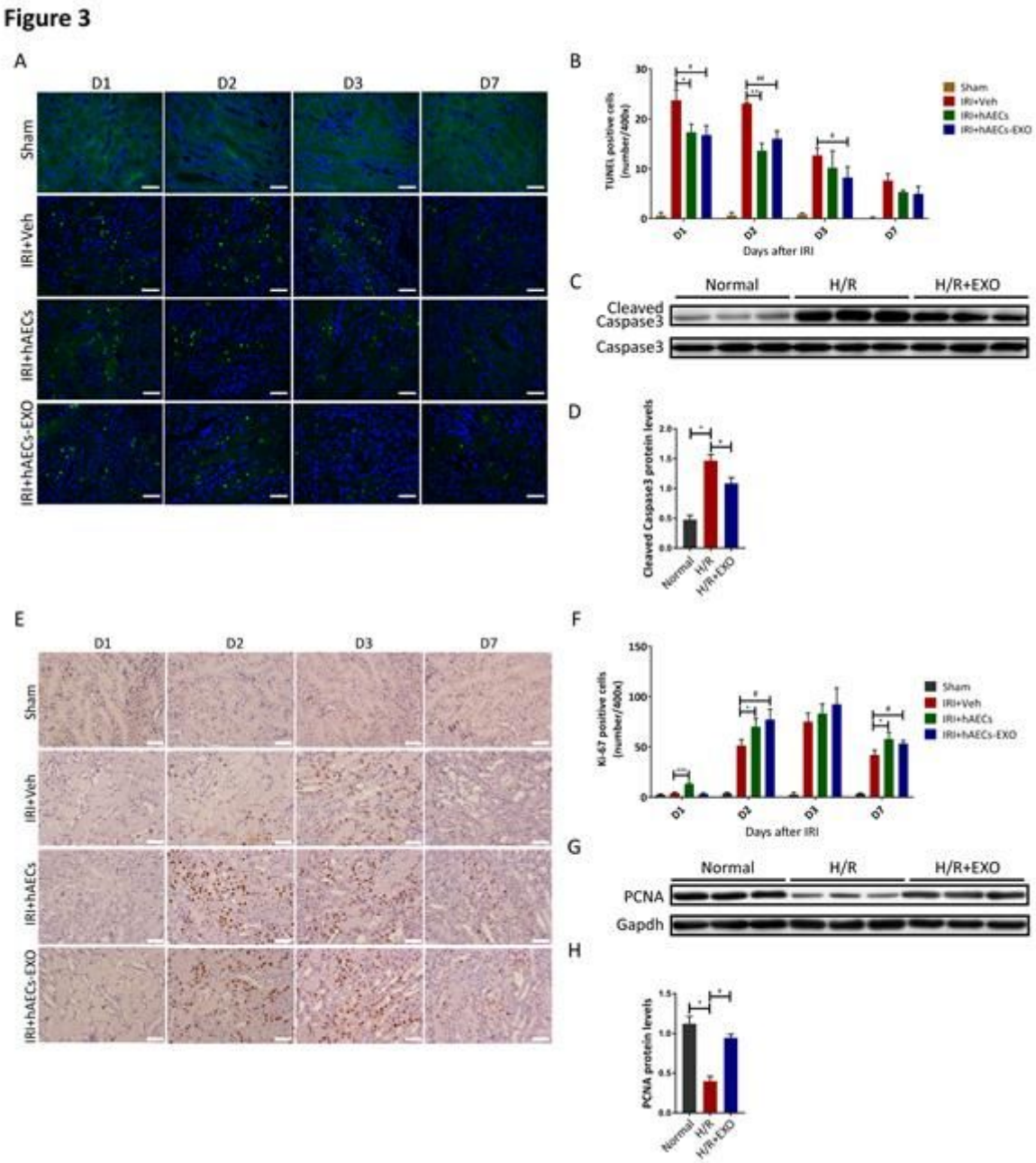

Figure 3

Anti-apoptotic effect of hAECs or hAECs-EXO in IRI mice and H/R injured HK2 cells. A, Representative micrographs of TUNEL staining in different groups as indicated at day 1, day 2, day 3 and day 7 postischemia. Scale Bar: 25 μm. B, Quantification of TUNEL-positive cells/HPF. 3 different mice were used in each group with at least 6 images were taken on each mouse kidney. *P < 0.05 vs IRI+Veh group; **P < 0.01 vs IRI+Veh group; #P < 0.05 vs IRI+Veh group; ## P < 0.01 vs IRI+Veh group. C, Representative Western blots showed protein expression of cleaved-caspase 3 and caspase 3 in different groups as indicated. D, Graphic presentation showed the relative abundances of cleaved-caspase 3 in different

groups. *P < 0.05 vs normal control; # P < 0.05 vs H/R group (n=3). E, Representative micrographs of Ki67 staining in different groups as indicated at day 1, day 2, day 3 and day 7 postischemia. Scale Bar: 25 μm. F, Quantification of Ki67 positive cells/HPF. 3 different mice were used in each group with at least 6 images were taken on each mouse kidney. *P < 0.05 vs IRI+Veh group; ***P < 0.001 vs IRI+Veh group; #P < 0.05 vs IRI+Veh group. G, Representative Western blots showed protein expression of PCNA in different groups as indicated. H, Graphic presentation showed the relative abundances of PCNA in different groups. *P < 0.05 vs normal control; # P < 0.05 vs H/R group (n=3).

Figure 4

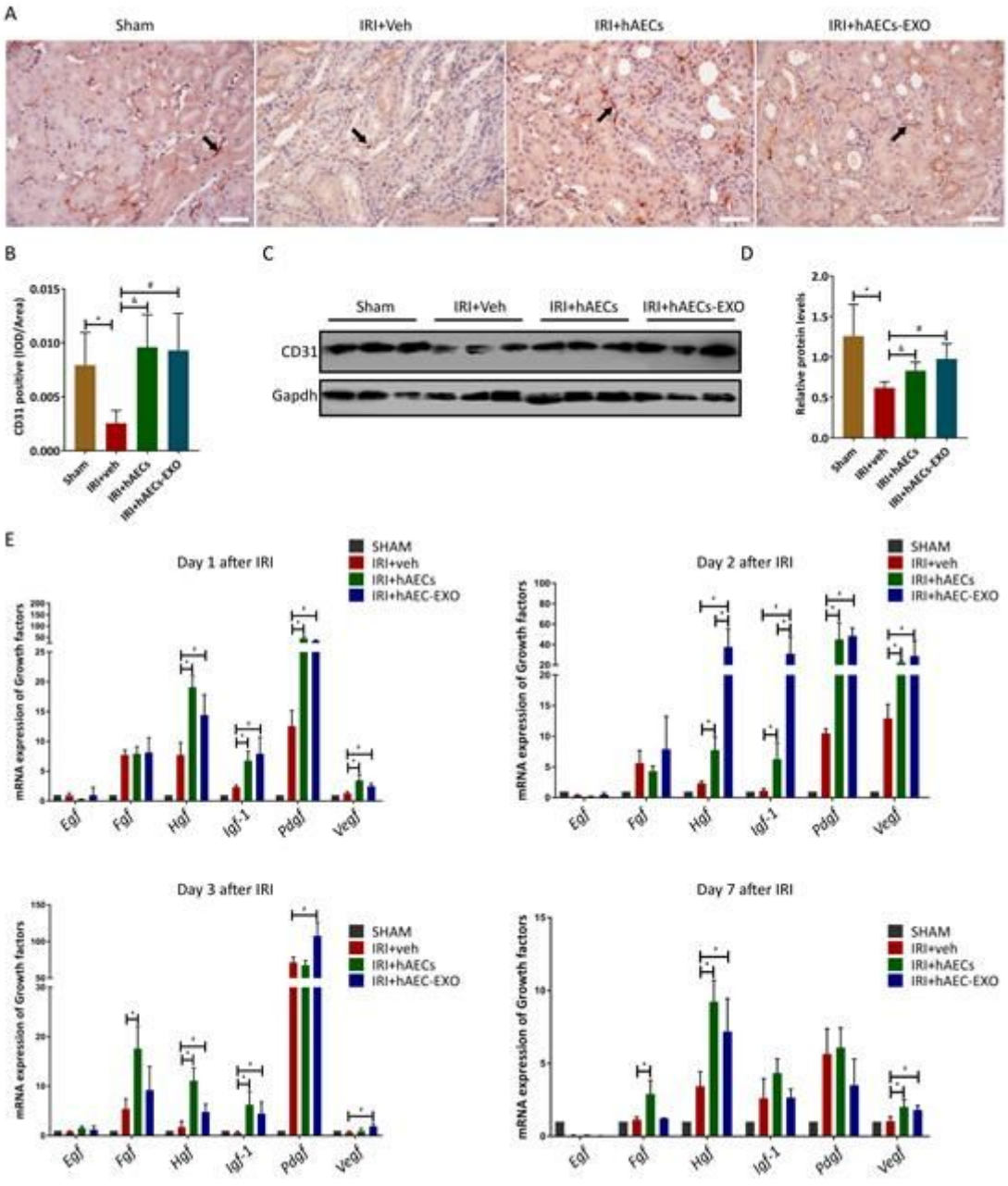

Figure 4

Pro-angiogenetic effect of hAECs or hAECs-EXO in mice with IRI-induced AKI. A, Representative micrographs of CD31 staining in different groups as indicated at day 7 postischemia. Arrows indicate

CD31 positive peritubular capillaries (PTCs). Scale Bar: 25 μm. B, Quantification of CD31-positive signal/HPF. 3 different mice were used in each group with at least 6 images were taken on each mouse kidney. *P < 0.05 vs sham group; &P< 0.05 vs IRI+Veh group; # P < 0.05 vs IRI+Veh group. C, Representative Western blot analyses showed protein expression of CD31 in different groups as indicated. D, Graphic presentation showed the relative abundances of CD31 in different groups. *P < 0.05 vs sham group; &P< 0.05 vs IRI+Veh group; # P < 0.05 vs IRI+Veh group (n=3). E. Growth factors expression in postischemic kidneys on day 1, day 2, day 3 and day 7 after hAECs or hAECs-EXO administration in mice with IRI-induced AKI. mRNA transcripts of Egf, Fgf, Hgf, Igf-1, Pdgf, Vegf were determined by qRT-PCR. * P < 0.05 vs IRI+Veh group; # P < 0.05 vs IRI+Veh group.

Figure 5

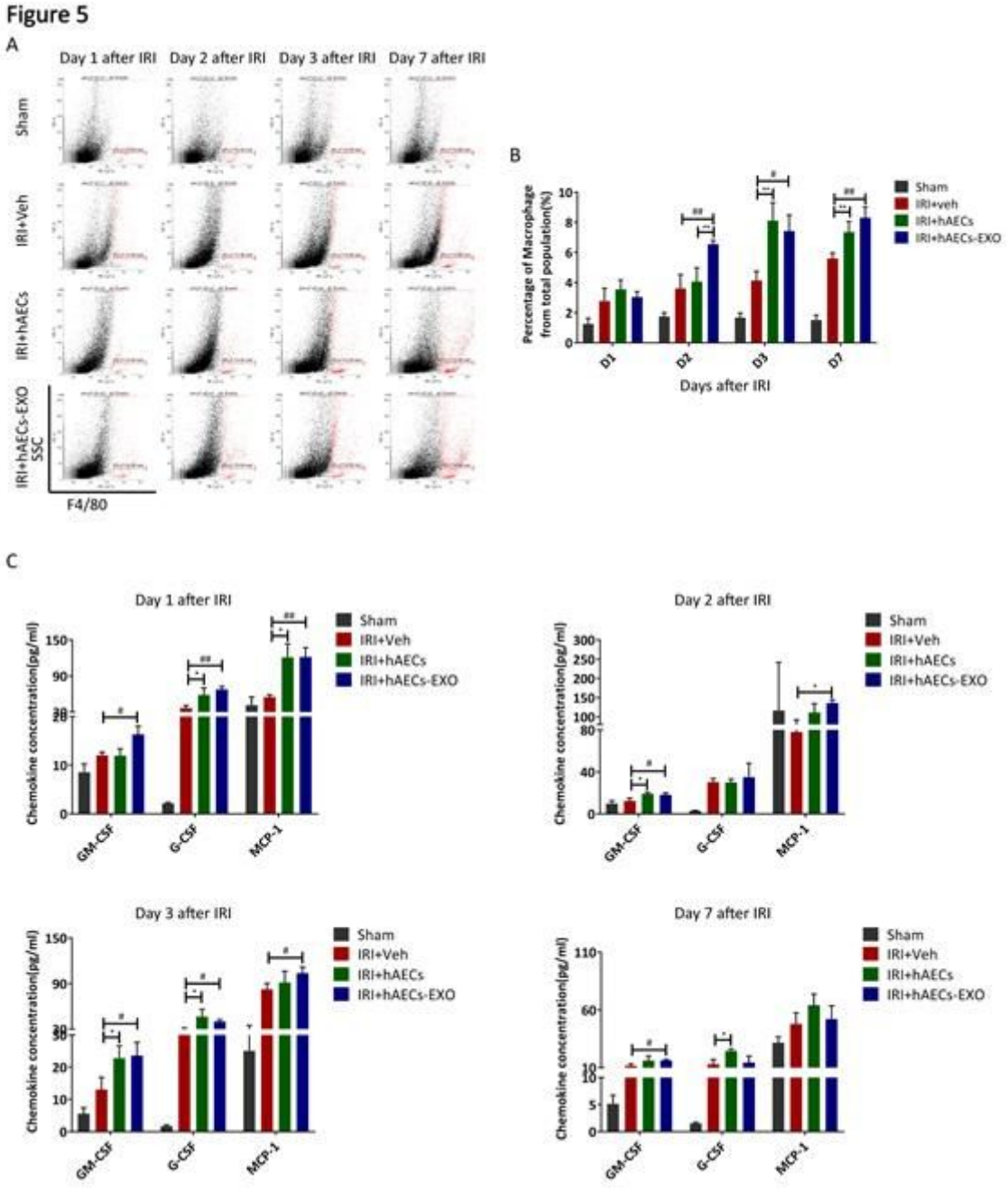

Figure 5

hAECs altered chemokine expression and macrophage infiltration in kidneys with IRI-induced AKI. A, Macrophage populations were measured via flow cytometry. Representative gating strategy was shown. The percentages of macrophages from the total kidney cell population were calculated. B, Percentage of F4/80+ macrophages in kidneys treated with hAECs or hAECs-EXO at day 1, day 2, day 3 and day 7 postischemia. **P < 0.01 vs IRI+Veh group; #P < 0.05 vs IRI+Veh group; ##P < 0.01 vs IRI+Veh group. C, Kidney chemokine concentrations from mice in different groups as indicated at day 1, day2, day 3 and day 7after IRI. *P < 0.05 vs IRI+Veh group; #P < 0.05 vs IRI+Veh group; ##P < 0.01 vs IRI+Veh group.

Figure 6

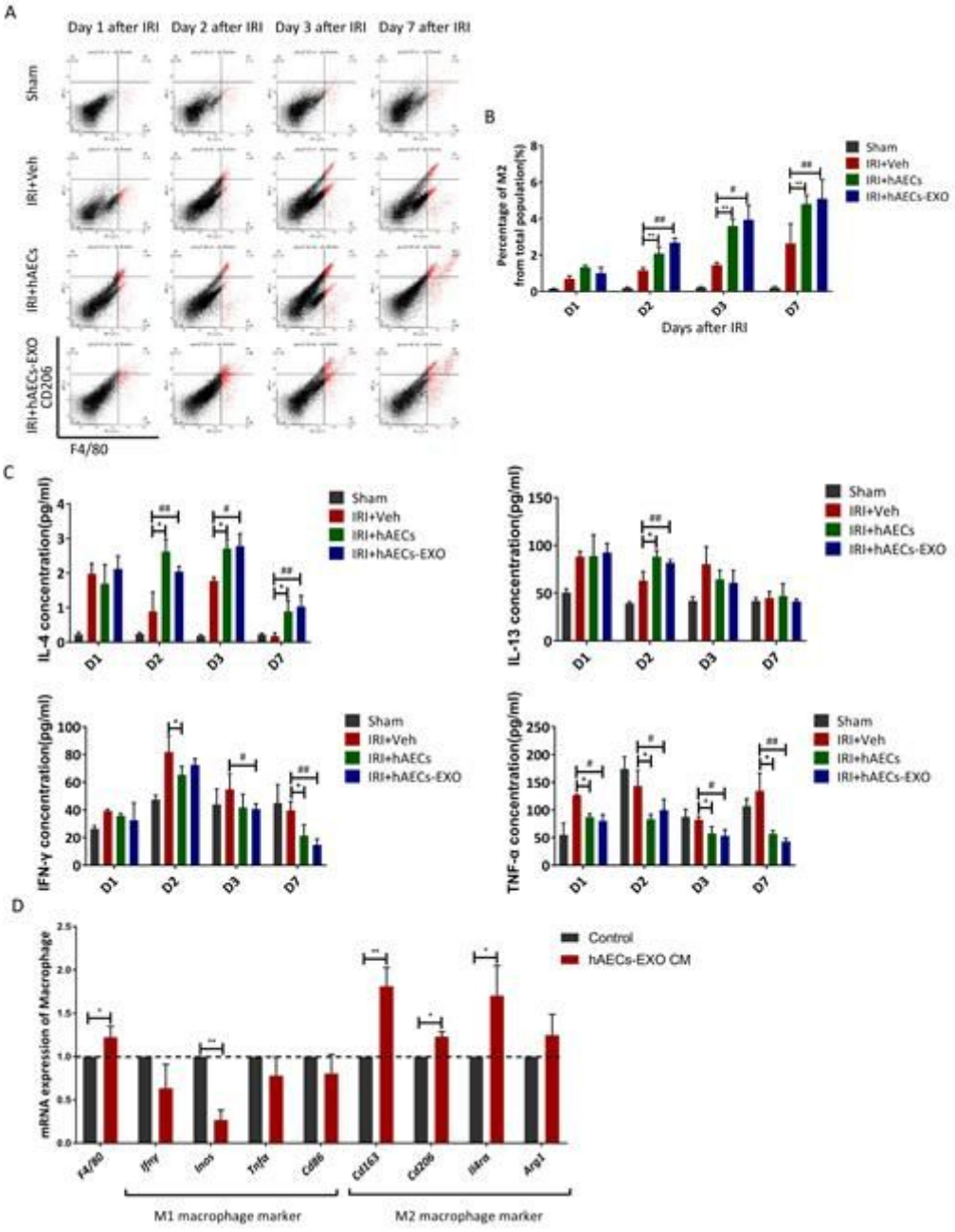

Figure 6

hAECs-EXO induced M2 macrophage polarization. A, CD206+/F4/80+ M2 macrophage population was measured via flow cytometry. Representative gating strategy was shown. The percentages of M2

macrophages from the total kidney cell population were calculated. B, Percentage of M2 Macrophages in kidneys treated with hAECs or hAECs-EXO at day 1, day 2, day 3 and day 7 postischemia. **P < 0.01 vs IRI+Veh group. #P < 0.05 vs IRI+Veh group; ## P < 0.01 vs IRI+Veh group. C, Kidney cytokine concentrations from mice in different groups as indicated at day 1, day2, day 3 and day 7 after IRI. *P < 0.05 vs IRI+Veh group; #P < 0.05 vs IRI+Veh group; ## P < 0.01 vs IRI+Veh group. D, Bone marrow monocytes were attached for 48h and collected as control. Bone marrow-derived macrophages were cultured in hAECs-EXO conditioned medium for 7 days and collected. mRNA transcripts of macrophage marker (F4/80) and M1 (Ifnγ, iNos, Tnfα, Cd86) and M2 (Cd163, Cd206, Il4rα, Arg1) markers were determined by qRT-PCR. * P < 0.05 vs control group; ** P < 0.01 vs control group. Data are shown as mean (SD).

Figure 7

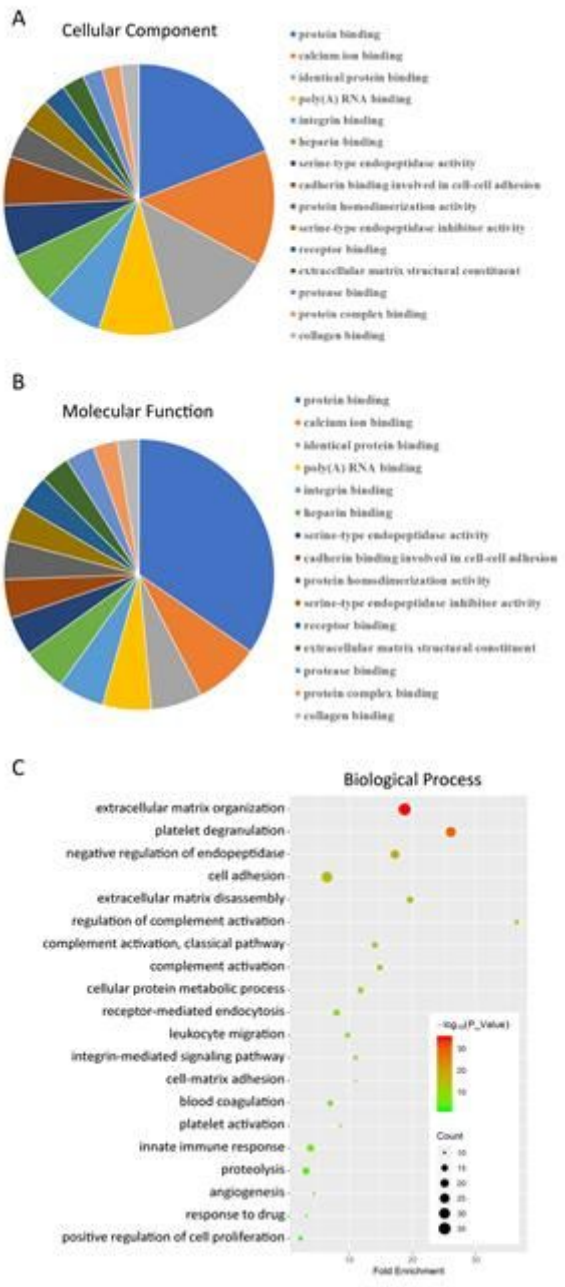

Figure 7

Proteomic profile of exosomes derived from hAECs. A and B, Gene ontology (GO) enrichment analysis for the significantly enriched GO terms of Cellular Component and Molecular Function. C, Bubble chart of the biological processes significantly enriched in hAECs exosome.

Supplementary Files

This is a list of supplementary files associated with this preprint. Click to download.

- hAECsonAKIsupplementarytable1.docx
- hAECsonAKIsupplementarytable2.xlsx
- SupplementaryFigure1.tif
- SupplementaryFigure2.tif